Molecular Crystals and Liquid Crystals

ISSN: 1542-1406 (Print) 1563-5287 (Online) Journal homepage: http://www.tandfonline.com/loi/gmcl20

Analysis of stress field in Al_2O_3-ZrO_2 biomaterials by finite element method

S. Laasri, M. Es-Sadik, M. Taha, A. Laghzizil, E.K. Hlil & A. Hajjaji

To cite this article: S. Laasri, M. Es-Sadik, M. Taha, A. Laghzizil, E.K. Hlil & A. Hajjaji (2016) Analysis of stress field in Al_2O_3-ZrO_2 biomaterials by finite element method, Molecular Crystals and Liquid Crystals, 627:1, 141-147, DOI: 10.1080/15421406.2015.1137130

To link to this article: http://dx.doi.org/10.1080/15421406.2015.1137130

Published online: 13 May 2016.

MOL. CRYST. LIQ. CRYST.
2016, VOL. 627, 141–147
http://dx.doi.org/10.1080/15421406.2015.1137130

Taylor & Francis
Taylor & Francis Group

Analysis of stress field in Al_2O_3-ZrO_2 biomaterials by finite element method

S. Laasri[a], M. Es-Sadik[b], M. Taha[b], A. Laghzizil[c], E.K. Hlil[d], and A. Hajjaji[a]

[a]Laboratoire des Sciences de l'Ingénieur pour l'Energie, Ecole Nationale des Sciences Appliquées d'El Jadida, BP 1166 EL Jadida Plateau 24002, Maroc; [b]Laboratoire de Thermodynamique et Energétique, Université Ibn-Zohr, Faculté des Sciences, BP 8106 Agadir Morocco; [c]Laboratoire de Chimie Physique Générale, Faculté des Sciences, Université Mohammed V-Agdal, BP.1014 Rabat Morocco.; [d]Institut Néel, CNRS et Université Joseph Fourier, BP 166,38042 Grenoble, France

ABSTRACT

We present an investigation of the mechanical properties of Al_2O_3-ZrO_2 as duplex-structured materials using the finite element method (FEM). The creation of stress fields are a result of the material trying to dissipate mechanical energy that is being exerted on the biomaterial. By finite element modelling and the stress fields, as either compressive or tensile, we can understand how inclusions interact with each other bioceramic lattice containing alumina in the presence of different zirconia contents. The stress fields can be applied to various strengthening mechanisms in bioceramic. They can be created by adding several inclusions in alumina lattice.

KEYWORDS

Bioceramic; Al_2O_2/ZrO_2; Mechanic properties; Finite element modelling; 2D reconstruction

1. Introduction

Bioceramics became an accepted group of materials for medical applications, mainly for implants in orthopaedics, maxillofacial surgery and for dental implants [1–3]. In the last years, layered configurations have been studied as a structural option for improving the mechanical behavior and reliability of ceramics. Presently, bioceramics have become a diverse class of biomaterials including three basic types: (i) bioactive ceramics as calcium phosphate that forms direct chemical bonded with bone or even with soft tissue of a living organism, (ii) bioresorbable (bioglass and glass ceramics) ceramics that actively participate in the metabolic processes of an organism, and (iii) bio-inert high strength ceramics such as alumina (Al_2O_3) and zirconia (ZrO_2). Zirconia is a most used biomaterial that has a higher mechanical strength and fracture toughness, while alumina is the most studied material for the implants development considered as low-cost with easily manipulation. Besides, it is widely used on numerous domains in particular in the orthopaedic applications. The combination of various bioceramics with the development of partially stabilized zirconia and alumina is the part of biomaterials world becoming increasingly important in medical devises. The mechanical properties of Al_2O_3-ZrO_2 bioceramic materials are largely discussed [1–4]. Contrary to alumina ceramic, the zirconia is a very interesting potential candidate for orthopaedic devices due to its exceptional mechanical properties such as the tenacity and fracture [1]. As disvantage, they can be

CONTACT S. Laasri laasrisaid@yahoo.fr

affected by ageing phenomenon in humid environment degrading their mechanical properties related to structural phase change from unstable tetragonal to the monoclinic stable phase [2–5]. For this aim, the addition of Al_2O_3 to ZrO_2 system is necessary to avoid the ageing process of zirconia [2–4]. Several mechanisms could jointly contribute to the improvement of the mechanical properties of these interesting composites such as reinforcement by micro-cracking, deviation or cracks decking [6]. In the addition porosity and number of defects and defect sizes are minimized using sintering step under inert gas pressure [7]. Generally as known, the natural cracks learn from the pre-existent defects and afterward tend to propagate in internal ceramic. To hinder their distribution, inclusions were introduced to toughen the ceramic matrix which keep the high values of hardness and flexion toughness and favor the micro-cracks by the introduced inclusions. By using a finite element method, we have studied the zirconia reinforcement in alumina matrix, involving the interaction between the field in frontage constraints of crack and the residual constraints around the reinforced zones. The influence of crack position and length on the dynamic characteristics of inclusions have been simulated and discussed. From such simulations, we are able to demonstrate that the crack position and crack length affect the gear's natural frequency as well as vibration shape.

2. Materials and methods

2.1. *Finite element model (FEM)*

The Cast3m calculations code is used in this work for structural analysis based on the finite element method. This code, developed by the Mechanical and Technology Department of Atomic Energy Commission (CEA-France), is widely used in fluid dynamics and materials science [8–10]. FEM is a numerical technique for finding approximate solutions to boundary value problems. Indeed, FEM encompasses accurate representation of complex geometry, inclusion of dissimilar material properties, easy representation of the total elucidation, as well as capture of local cracks effects to solve complex elasticity. The finite elements implanted in the software are of linear chap, quadratic in one (1D), two (2D), and three (3D) dimensions. However, this software does not have an interface, what makes their manipulation more difficult.

2.2. *Materials*

The finite element modelling provides detailed information regarding the development of stress fields associated with several inclusions. In this way, it becomes possible to analyze the micro-cracks inside the Al_2O_3 bio-ceramic. The modelling conditions are: (a) Matrix in alumina, (b) Inclusion of Al_2O_3+x%.ZrO_2 (noted AZ_x), *(c)* The inclusion effect on the matrix likened to an internal pressure with their values depends on the zirconia content in the reinforcement zone, (d) The inter-inclusion distance depends on the inclusion percentage in matrix volume, (e) The mechanical and geometrical properties are taken according to those reported by Lutz et al. [11–12].

2.3. *Meshes and boundary conditions*

The meshes are created by quadrilateral elements with 8 nodes in 2 dimensions (figure 1).The material behavior is elastic isotropic.

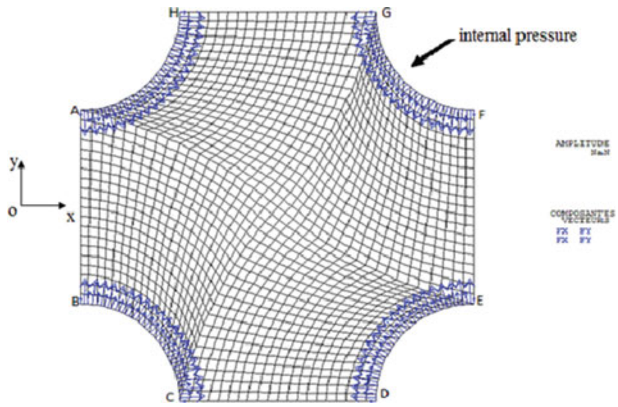

Figure 1. Meshes and boundary conditions.

Table 1. Materials properties [14].

Properties	Young modulus	Poisson ratio	density	tensile strength
Alumina	360 GPa	0.21	3.8 g/cm^3	1000 MPa

The properties of material are illustrated in the Table 1:
Boundary conditions are applied as follows (figure 1):

- Lines AB and EF are blocked in the X direction.
- Lines CD and HG are blocked in the Y direction
- The all surface is blocked in the z direction.

3. Results and discussions

During the ceramic cooling, some zones in bio-ceramic dilate with zirconia content. Here, we present a numerical study of the stress fields around spherical inclusions Al_2O_3-x%ZrO_2, where x is the of zirconia contenting reinforcement zone (Figure 2). The finite element modelling takes into account the experimental studies carried out by Lutz and coll. [11] on ceramic samples. If zones B are the phase transformation or thermal expansion related to the difference in dilation and thermal coefficients ε_V in reinforcement Al_2O_3 matrix, the expansion in volume, according to eaquation reported by Lutz and coll. [12] is: $[\varepsilon_V = \frac{\Delta V}{V} + 3.(\alpha_A - \alpha_B).\Delta T]$, where $[\frac{\Delta V}{V}]$ represents the variation in volume related to the transformation phase ZrO_2 (zone

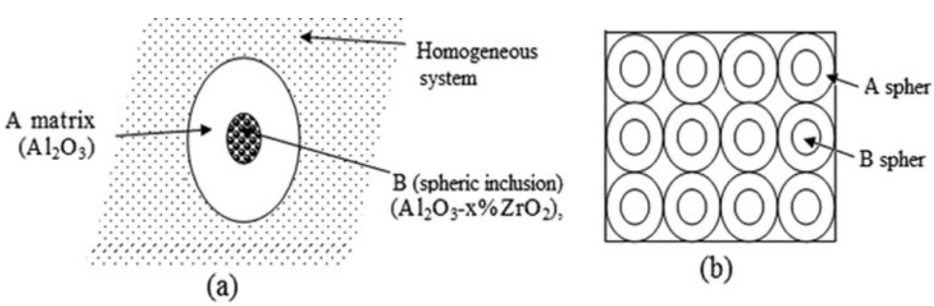

Figure 2. (a) Duplex structure, (b) Duplex structure according to Lutz.

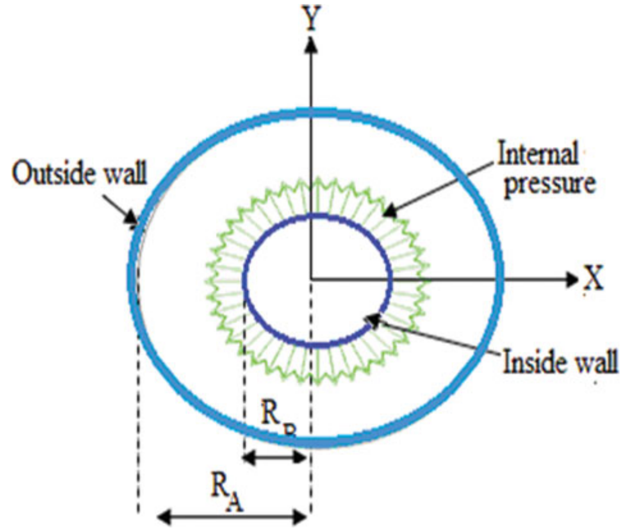

Figure 3. Description of the studied geometry.

B), [$\alpha_A$andα_B] are thermal dilatation coefficients of A and B spheres, respectively. The [ΔT] is the temperature deviation in the considered conditions.

The pressure with the interface inclusion-matrix is expressed as:

$$P_{iso}^{B} = -C.\left(1-\left(\frac{r^B}{r^A}\right)^3\right) \quad (1)$$

Where

$$C = \frac{1/2E_A.E_B.\varepsilon^V}{2E_A.(1-2\nu_B)+E_B(1+\nu_A)+[2.E_B.(1-2\nu_A)-E_A(1-2\nu_B)](\frac{R_B}{R_A})^3}$$

With (E_A and E_B), (V_A and V_B) and (R_A and R_B) are the Young's Modulus, Poisson coefficients and inter-inclusion for A and B, respectively.

The spherical inclusion effect is compared to an internal pressure that its value depends on the zirconia content in each inclusion. The figure 3 shows the scheme for the used geometrical matrix for internal pressure calculations.

According to the conditions considered by Lutz [13], the calculated pressures for optimum Al_2O_3-x%ZrO_2 ceramics are reported in figure 4.This internal pressure decreases when the R_B/R_A ratio increases. However, this pressure also increases with zirconia content such as reported elsewhere [15].Then, we conclude that Al_2O_3-35%ZrO_2 bioceramic is considered as the most selected zirconia content in view of suitable rupture with lower internal pressure than 1000 MPa [14].

From finite element construction applied on the quadratic system at four nodes, the figure 5 shows the internal pressure effect on the cylindrical plate, which confirms that the pressure field is radial with an increase of the principal constraint with ZrO_2 content such as reported elsewhere [1–3].Consequently, the reinforcement in ceramic containing alumina and zirconia compounds is related to the interaction between the stress field in frontal crack and the residual stress fields around spherical inclusions. However, the elastic energy stored around the spherical zones should not exceed the propagation energy of cracks [16]. Based on Selsing and Lundin models, Lutz [11] calculated the radial and tangential constraints around spherical inclusions. He considers that the duplex structure includes a spherical and dense

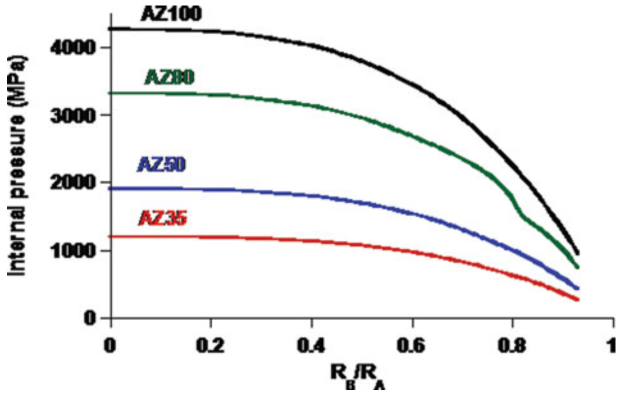

Figure 4. Internal pressures for Al_2O_3-x%wt.ZrO_2 inclusion as the function of R_B/R_A.

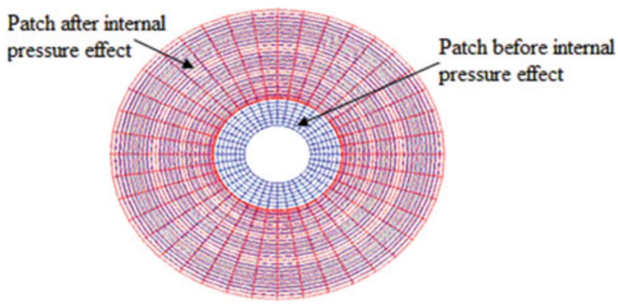

Figure 5. Typical patch before and after internal pressure effect.

implement, which wrap other small sphere B (Figure 1b).From results computed by the finite element method (Figure 6) applied to 65% Al_2O_3-35%ZrO_2 ceramic, the first stress field is very intense in frontal inclusion and decreases quickly towards zero value in extreme cases of the cylindrical plate. Additionally, this stress field decreases by increasing the inclusion size. From this result point of view, we consider that a good correlation with results given by the continuous fluid dynamics is established.

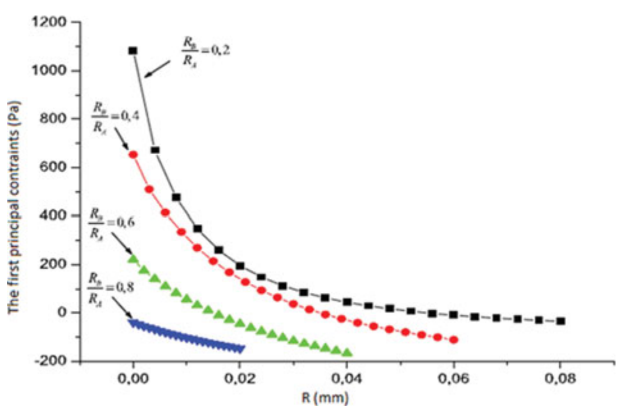

Figure 6. Distribution of the 1st principal constraints as the function R_B/R_A for the case or inclusion is made up of 75% from Al_2O_3 and 35% of ZrO_2 (AZ35).

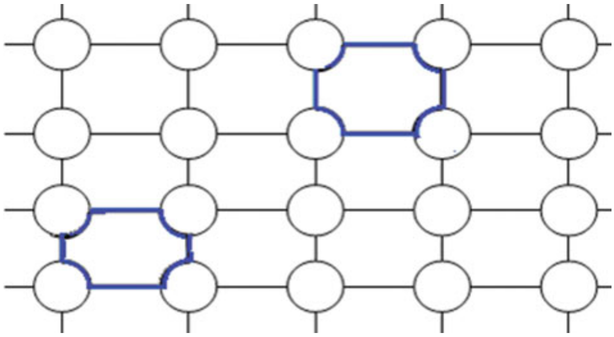

Figure 7. Schematic figure showing the regular matrix.

To solve the created stress field around a number of spherical inclusions by finite element method, the inter-inclusion distance was varied to amplify ceramic matrix during the deformation in alumina ceramic with the presence of hot working zirconia. Therefore, the morphology of inclusions in wrought ceramics is largely controlled by their mechanical behavior during the thermal processing. To simplify this investigation, the scattered network of inclusions by a squared regular matrix has been opted (Figure 7).

Initially, we limited our calculations only to four inclusions dispersed at the tops of the elementary square. In this case, the internal pressure values also depend on the zirconia content with 32 μm as inclusion diameter. The typical behaviors of different types of inclusions during the deformation are schematically given in Figure 8.

From figure 8, we note that the reduction in inter-inclusions distance (black zones) involves the increase in compression (blue network). So, in the restricted blue zone if the constraint is low or almost zero, the deviation of a crack, which is propagated in the matrix will not take place where the distance inter-inclusions is higher than 140 μm for the dispersion of inclusions containing $65\%Al_2O_3+35\%ZrO_2$ in an alumina matrix.

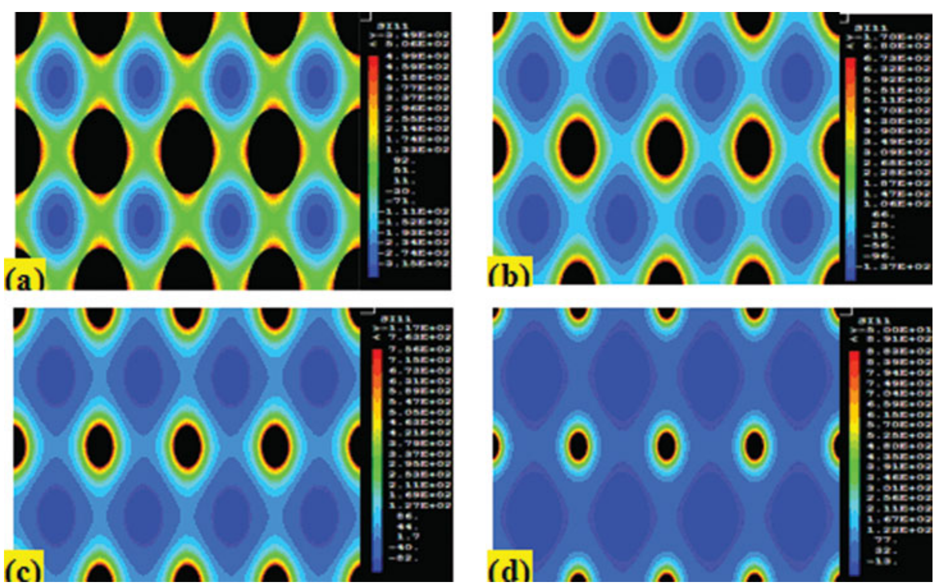

Figure 8. Distribution of the first main stress field near of various inter-inclusion distances « d ». (a) d = 40 μm, (b) d= 100 μm, (c), d = 140 μm, (d) d = 260 μm.

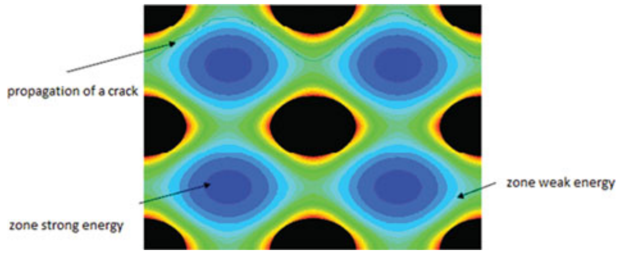

Figure 9. Example of deviation of a crack in a plate containing of inclusions.

Figure 9 shows an example of a crack deviation propagated in one stamp out of alumina containing spherical inclusions. The cracks are propagated in the zones of weak energies with a deviation of the cracks induced by skirting of the black spherical zones and zones put in compression in blue. Similar phenomenon was already observed in experiments reported by Lutz [11–13].

4. Conclusion

We have used the finite element method to study the distribution of the principal stress fields in Al_2O_3-ZrO_2 matrix with several inclusions. Results show that the reinforcement is ensured by the transformation of zirconia phase in the reinforcement zones. In addition, the principal stress fields are influenced by the residual stress field around inclusions. This residual stress field is very high at inclusion-matrix interface.

Consequently, the developed model led to optimize the inter-inclusion distance and allows the crack deviation propagated in alumina matrix.

References

[1] Liu, G. J., Qiu, H. B., Todd, R., Brook, R. J., & Guo, J. K. (1998). *Mat. Res. Bulletin*, *33*, 281–288.
[2] Claussen, N. (1976). *J. Am. Ceram. Soc.*, *59*, 49–51.
[3] Lee, B. T., Kang, I. C., Gain, A. K., Kim, K. H., & Song, H. Y. (2006). *Journal of the European Ceramic Society*, *26*, 3525–3530.
[4] Basu, D., Das Gupta, A., Basu, M. K., & Sakar, B. K. (1996). *J. Euro. Ceram. Soc.*, *16*, 613–617.
[5] Lutz, H. E., & Claussen, N. (1991). *J. Euro. Ceram. Soc.*, *7*, 219–226.
[6] Claussen, N., Steeb, J., & Pabst, R. F. (1977). *J. Am. Ceram. Soc.*, *56*, 559–562.
[7] Claussen, N., Ruhle, M., & Heuer, A. H. (1984). In *Science & Technology of Zirconia II*, American Ceramic Society, Columbus, 64–77.
[8] http://www-cast3m.cea.fr/
[9] Yu, T., Liu, X., Ye, J., & Zhang, M. (2014). *Ceramics International*, *40*, 2933–2942.
[10] Han, X. (2015). *Modelling Degradation of Bioresorbable Polymeric Medical Devices*, *113–130*, 131–140.
[11] Lutz, H. E., & Swain, M. V. (1992). *J. Amer. Ceram. Soc.*, *75*, 1729–1736.
[12] Lutz, H. E., Swain, M. V., & Claussen, N. (1991). *J. Amer. Ceram. Soc.*, *74*, 19–24.
[13] Lutz, H. E., & Claussen, N. (1991). *J. Euro. Ceram. Soc.*, *7*, 209–218.
[14] Taha, M. (1993). *Elaboration et caractérisation de poudres de zircones, Thesis*, INSA-Lyon France.
[15] Laasri, S., Taha, M., Hlil, E. K., & Hajjaji, A. (2011). *C. R. Mecanique*, *339*, 35–41.
[16] Olagnon, C., Chevalier, J., & Pauchard, V. (2006). *Journal of the European Ceramic Society*, *26*, 3051–3059.